

A CONFORMALIZED LEARNING OF A PREDICTION SET WITH APPLICATIONS TO MEDICAL IMAGING CLASSIFICATION

Roy Hirsch Jacob Goldberger

Faculty of Engineering, Bar-Ilan University, Ramat-Gan, Israel
jacob.goldberger@biu.ac.il

ABSTRACT

Medical imaging classifiers can achieve high predictive accuracy, but quantifying their uncertainty remains an unresolved challenge, which prevents their deployment in medical clinics. We present an algorithm that can modify any classifier to produce a prediction set containing the true label with a user-specified probability, such as 90%. We train a network to predict an instance-based version of the Conformal Prediction threshold. The threshold is then conformalized to ensure the required coverage. We applied the proposed algorithm to several standard medical imaging classification datasets. The experimental results demonstrate that our method outperforms current approaches in terms of smaller average size of the prediction set while maintaining the desired coverage.

Index Terms— neural networks, interpretability, prediction sets, calibration, conformal prediction

1. INTRODUCTION

Deep learning holds immense potential for automating numerous clinical tasks in medical imaging. However, the translation of black-box deep learning procedures into clinical practice has been impeded by the absence of transparency and interpretability. Many clinical deep learning models lack rigorous, robust techniques for conveying their confidence in their predictions, which limits their appeal for widespread use in medical decision-making. In the case of medical imaging classification tasks, in addition to the most likely diagnosis, it is equally or more important to rule out options. Decision reporting in terms of a prediction set of class candidates is thus a natural approach for clinical applications. In this procedure, most classes are ruled out by the network, leaving the physician with only a few options to further investigate. In terms of confidence, we expect that the prediction set provably covers the true diagnosis with a high probability (e.g., 90%).

Conformal Prediction (CP) [1, 2] is a general non-parametric calibration method that was initially formulated for the task of classification, and was later modified for regression. In the case of classification, given a confidence level

$1 - \alpha$, it aims to build a small prediction set with a guarantee that the probability that the correct class is within this set is at least $1 - \alpha$. CP was invented more than twenty years ago, before deep learning have emerged. Recently, it has become a major calibration tool for neural network systems in various applications including medical imaging [3, 4]. CP is not a specific algorithm but rather a general framework in which selecting a specific conformal score (aka non-conformity score) defines the way the prediction set is constructed. The parameters of the CP algorithm are tuned on a validation set to ensure the required coverage of the prediction set. To make CP effective, the size of the prediction set should be as small as possible. The effectiveness of different CP variants is thus measured by calculating the average size of the prediction sets on the test set.

Note that in addition to the CP calibration algorithm, which focuses on forming a prediction set with guaranteed coverage, there is another family of calibration algorithms whose goal is to tune the confidence of the predicted class. The most widely used strategy is post-hoc calibration of the softmax logit scores, e.g., Temperature Scaling [5, 6]. Here, the calibration goal is different in that it involves forming a small but reliable prediction set.

The Adaptive Prediction Sets (APS) score, which was first introduced in [7], is a commonly used conformal score. The APS algorithm generates a prediction set by selecting the most likely classes until the cumulative probability exceeds a predetermined threshold. The Regularized Adaptive Prediction Sets (RAPS) algorithm [8] is a variant of the APS method that modifies its conformal score by penalizing prediction sets that are too large. This approach is particularly useful for classification tasks with many possible labels. It returns predictive sets that achieve a pre-specified error level while retaining a small average set size. All current CP variants, including APS and RAPS, are based on finding a single threshold, denoted as q , such that the conformal scores of most of the validation-set samples are below q . This implies that for some of the samples, q is overly pessimistic, leading to unnecessarily large prediction sets.

In this study, we introduce a CP algorithm in which the threshold used to create the prediction set is optimized for each sample individually. The threshold is computed by a

This research was supported by the Ministry of Science & Technology, Israel.

neural network and then adjusted (conformalized) to ensure that it meets the coverage requirements. We applied the proposed algorithm to several standard medical imaging classification datasets. The experimental results demonstrate that our method outperforms existing state-of-the-art CP methods significantly, in terms of the average size of the prediction set while maintaining the same coverage.

2. CONFORMAL PREDICTION

In this section we review the commonly used variants of the Conformal Prediction algorithm [1] and in the next section we present our approach within this framework.

Consider a network that classifies an input x into k pre-defined classes. Given an input x with an unknown class y we want to find a small prediction set of classes $C(x) \subset \{1, \dots, k\}$ such that $p(y \in C(x)) > 1 - \alpha$ where α is a pre-defined miss-coverage rate. A simple approach to achieving this goal is to include classes from the highest to the lowest probability until their sum just exceeds the threshold $1 - \alpha$. As in [8], this uncalibrated prediction-set strategy is dubbed here ‘naive’. While the network output has the mathematical form of a distribution, this does not necessarily imply that it represents the true class distribution. The network is usually not calibrated and tends to be over-optimistic [5].

The CP algorithm builds a prediction set (with a probabilistic justification) in the following way. Let x be a sample along with its network-based class probabilities p_1, \dots, p_k . Let $\pi(x)$ be the permutation of $\{1, \dots, k\}$ sorted from the most likely class to the least likely, i.e.

$$p(\pi_1) \geq \dots \geq p(\pi_k).$$

For each $v \in [0, 1]$ we form the prediction set $C_v(x)$ by taking top-scoring classes until the total mass just exceeds v . More formally, $C_v(x) = \{\pi_1(x), \dots, \pi_l(x)\}$ such that:

$$l = \min\{l' \mid \sum_{i=1}^{l'} p(\pi_i) \geq v\}. \quad (1)$$

Given a labeled sample (x, y) s.t. $y \in \{1, \dots, k\}$, the Adaptive Prediction Score (APS) [7] is defined to be the set of all the classes whose score is greater or equal to the score of the true label y :

$$s(x, y) = \sum_{\{i \mid p_i \geq p_y\}} p_i \quad (2)$$

The score $s(x, y)$ is the minimal $v \in [0, 1]$ in which the true class y is in a prediction set $C_v(x)$. We can define a randomized version of (2) as follows:

$$s_{\text{random}}(x, y) = u \cdot p_y + \sum_{\{i \mid p_i > p_y\}} p_i \quad (3)$$

s.t. u is a r.v. uniformly distributed in the interval $[0, 1]$. The randomization can help to achieve $1 - \alpha$ coverage exactly on

Algorithm 1 Conformalized Prediction Set Network (CPSN)

Training Phase:

- 1: Given a training set $(x_1, y_1), \dots, (x_n, y_n)$, calculate the APS conformal score per instance $s(x_t, y_t)$.
- 2: Learn a network $q(x; \theta)$ by minimizing the MSE loss:

$$l(\theta) = \sum_t (q(x_t; \theta) - s(x_t, y_t))^2.$$

Conformalization Phase:

- 1: Given a validation set $(x_1, y_1), \dots, (x_n, y_n)$, predict the conformal score per instance $q(x_t; \theta)$.
- 2: Define

$$\mathbb{G}_1 = \{r_t \mid \hat{p}(x_t) > 1 - \alpha\}, \quad \mathbb{G}_2 = \{r_t \mid \hat{p}(x_t) \leq 1 - \alpha\}$$

$$\text{s.t. } r_t = s(x_t, y_t) - q(x_t) \text{ and } \hat{p}(x_t) = \max_i p(y_t = i \mid x_t).$$

- 3: Define: $\delta_i = \lceil (n+1)(1-\alpha)/n \rceil$ -quantile of \mathbb{G}_i , $i = 1, 2$

Usage: Given a test sample x :

- 1: If $\hat{p}(x) > 1 - \alpha$ define $\delta(x) = \delta_1$ and otherwise $\delta(x) = \delta_2$.
- 2: Report the prediction set $C_{(q(x)+\delta(x))}(x)$.

There is a guarantee: $p(y \in C_{(q(x)+\delta(x))}(x)) \geq 1 - \alpha$.

the validation set [9]. The Regularized Adaptive Prediction Sets (RAPS) score [8] is a variant of APS that encourages small prediction sets. It is defined as follows:

$$s(x, y) = \sum_{\{i \mid p_i \geq p_y\}} (p_i + a \cdot 1_{\{i > b\}}) \quad (4)$$

s.t. a and b are parameters that needed to be tuned.

Let $(x_1, y_1), \dots, (x_n, y_n)$ be a labeled validation set and let $s_t = s(x_t, y_t)$ be the conformal score of (x_t, y_t) . s_t is the minimal threshold in which the true class y_t is in a prediction set of x_t . Let q be the $(1 - \alpha)$ quantile of s_1, \dots, s_n , i.e. if we sort the values $s_1 \leq \dots \leq s_n$ then $q = s_{(1-\alpha)n}$. The threshold q is the minimal one in which the correct label y_t is included in the prediction set $C_q(x_t)$ for at least $(1 - \alpha)n$ points of the validation set. Given a new test point x , we report the prediction set $C_q(x)$. The general CP theory [1] guarantees that:

$$1 - \alpha \leq p(y \in C_q(x)) \leq (1 - \alpha) + \frac{1}{n + 1},$$

where y is the unknown true label. Note that this is a marginal probability over all possible test points and is not conditioned on a given input.

3. AN INSTANCE-BASED THRESHOLD FOR A PREDICTION SET

Standard CP algorithms such as APS find and apply a single threshold to generate the prediction set for all the test sam-

| Model | OrganAMNIST | | | | TissuMNIST | | | |
|-----------|---------------------|-------------|---------------------|-------------|---------------------|-------------|---------------------|-------------|
| | $\alpha = .1$ | | $\alpha = .05$ | | $\alpha = .1$ | | $\alpha = .05$ | |
| | Size ↓ | Coverage | Size ↓ | Coverage | Size ↓ | Coverage | Size ↓ | Coverage |
| Naive | 2.646 ± .031 | .950 ± .003 | 3.444 ± .054 | .971 ± .003 | 2.678 ± .020 | .945 ± .003 | 3.339 ± .019 | .973 ± .002 |
| APS | 4.096 ± .059 | .899 ± .005 | 5.179 ± .071 | .952 ± .004 | 3.464 ± .031 | .899 ± .006 | 4.337 ± .037 | .949 ± .004 |
| Rand APS | 2.289 ± .030 | .922 ± .004 | 3.005 ± .033 | .958 ± .004 | 2.335 ± .023 | .912 ± .005 | 2.956 ± .023 | .953 ± .004 |
| RAPS | 2.586 ± .027 | .947 ± .003 | 3.325 ± .040 | .968 ± .003 | 2.676 ± .021 | .944 ± .004 | 3.318 ± .018 | .972 ± .003 |
| Rand RAPS | 2.259 ± .033 | .900 ± .006 | 2.977 ± .035 | .950 ± .003 | 2.319 ± .021 | .898 ± .005 | 2.944 ± .025 | .948 ± .003 |
| CPSN | 2.251 ± .034 | .935 ± .005 | 2.818 ± .073 | .964 ± .003 | 2.210 ± .023 | .906 ± .003 | 2.761 ± .020 | .953 ± .003 |

Table 1: Results on **OrganAMNIST** and **TissuMNIST** datasets. We report coverage and size for each model for two α values. We ran each experiment 10 times with different random splits and report the mean and standard deviation. For each setup, the best-performing results are bolded.

ples. We next present an instance-based CP version where a parametric model is used to predict a different threshold for each sample. We hypothesize that a per-sample threshold will enable us to generate smaller and therefore more informative prediction sets.

We first train a neural network to predict the APS score $s(x, y)$ (2) directly from the feature input vector x , without using the true class y . Given a training set $(x_1, y_1), \dots, (x_n, y_n)$, we learn a regression network by minimizing the following Mean Squared Error (MSE) loss:

$$l(\theta) = \sum_t (q(x_t; \theta) - s(x_t, y_t))^2 \quad (5)$$

such that θ is the network parameter set and $q(x_t; \theta)$ is the network output.

Since $q(x)$ is learned by a network it is not guaranteed to satisfy the α miss-coverage requirement. We next conformalize the learned threshold to obtain the required coverage. Assume we have a labeled validation set $(x_1, y_1), \dots, (x_n, y_n)$. Define the following conformity score as the residual:

$$r_t = s(x_t, y_t) - q(x_t), \quad t = 1, \dots, n. \quad (6)$$

For each t , $s(x_t, y_t)$ is the minimum value v such that $y_t \in C_v(x_t)$. Therefore, r_t is the minimal value (either positive or negative) such that $y_t \in C_{(q(x_t)+r_t)}(x_t)$. The residual scores act differently for predictions with higher and lower confidence levels. Hence, we can separate them into two sets based on whether the prediction confidence $\hat{p}(x) = \max_i p(y = i|x)$ is larger or smaller than $1 - \alpha$. We calculate the $(1 - \alpha)$ quantile for each of the two sets of scores and define a function $\delta(x)$ that returns the appropriate quantile given the maximal prediction probability. The bias correction function $\delta(x)$ enforces the conformity of the method.

Finally, given a test sample x we report the following prediction set: $C_{q(x)+\delta(x)}(x)$. In other words, we form the prediction set by summing the probabilities of the highly scored classes until we reach $q(x) + \delta(x)$. The general CP theory [2] guarantees that:

$$1 - \alpha \leq p(y \in C_{q(x)+\delta(x)}(x)) \leq (1 - \alpha) + \frac{1}{n + 1}, \quad (7)$$

where y is the unknown true label and n is the size of the validation set. As in other CP algorithms, this is a marginal probability over all possible test points and is not conditioned on a given input. The resulting method, which we call Conformalized Prediction Set Network (CPSN), is summarized in Algorithm Box 1.

4. EXPERIMENTAL RESULTS

In this section we report the performance of the proposed CPSN method on several publicly available medical imaging classification tasks.

Datasets. We used the **OrganAMNIST** and **TissuMNIST** datasets from the MedMNIST repository [10, 11]. **OrganAMNIST** is a dataset of Abdominal CT images with 11 body-organ classes. It is based on 3D CT images from Liver Tumor Segmentation Benchmark (LiTS) [12]. 2D images were cropped from the center slices of the 3D bounding boxes in axial views and resized into 28×28 . The dataset contains 58,850 images. The **TissueMNIST** dataset contains 236,386 human kidney cortex cells, organized into 8 categories. Each gray-scale image is $32 \times 32 \times 7$ pixels, where 7 denotes 7 slices. The 2D projections were obtained by taking the maximum pixel value along the axial-axis of each pixel, and were resized into 28×28 gray-scale images [13].

To generate the input features (x) and class probabilities (p), we utilized trained CNNs published by MedMNIST authors [10, 11]. Each classifier is a ResNet-50 [14] that has been fine-tuned over the train fold of one of the datasets. The logits/class probabilities as well as the pre-logits representation for each item were extracted from the validation and test sets. This results in 24,269 samples for the OrganAMNIST dataset and 70,920 samples for the TissueMNIST dataset.

Compared methods. We compared the proposed CPSN method to the following prediction-set generation procedures: 1) The ‘naive’ uncalibrated method [8] (see a description in Section 2). 2) The APS method [7] with and without a randomized procedure. 3) The RAPS method [8] with and without a randomized procedure.

Evaluation Measures. The primary measure used for the

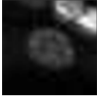



| | TissueMNIST | | OrganAMNIST | |
|------------------|--|---|--|---|
| | Labels = {Collecting Duct, Connecting Tubule (<i>C</i>), Distal Convolutated Tubule (<i>DCT</i>), Glomerular Endothelial Cells (<i>GEC</i>), Interstitial Endothelial Cells (<i>IEC</i>), Leukocytes (<i>L</i>), Podocytes (<i>P</i>), Proximal Tubule Segments (<i>PTS</i>), Thick Ascending Limb (<i>TAL</i>)} | | Labels = {Bladder (<i>B</i>), Femur Left (<i>FL</i>), Femur Right (<i>FR</i>), Heart (<i>H</i>), Kidney Left (<i>KL</i>), Kidney Right (<i>KR</i>), Liver (<i>L</i>), Lung Left (<i>LL</i>), Lung Right (<i>LR</i>), Pancreas (<i>P</i>), Spleen (<i>S</i>)} | |
| |  |  |  |  |
| Naive | { <i>C</i> , <i>PTS</i> , <i>TAL</i> } | { <i>IEC</i> , <i>C</i> , <i>PTS</i> , <i>L</i> , <i>P</i> , <i>DCT</i> } | { <i>KL</i> , <i>B</i> , <i>S</i> , <i>LL</i> } | { <i>B</i> , <i>KL</i> , <i>S</i> , <i>KR</i> } |
| APS | { <i>C</i> , <i>PTS</i> , <i>TAL</i> } | { <i>IEC</i> , <i>C</i> , <i>PTS</i> , <i>L</i> , <i>P</i> , <i>DCT</i> } | { <i>H</i> , <i>P</i> , <i>KL</i> , <i>B</i> , <i>S</i> , <i>LL</i> } | { <i>FR</i> , <i>LR</i> , <i>P</i> , <i>B</i> , <i>KL</i> , <i>S</i> , <i>KR</i> } |
| Rand APS | { <i>C</i> , <i>PTS</i> , <i>TAL</i> } | { <i>C</i> , <i>PTS</i> , <i>L</i> , <i>P</i> , <i>DCT</i> } | { <i>KL</i> , <i>B</i> , <i>S</i> , <i>LL</i> } | { <i>KL</i> , <i>S</i> , <i>KR</i> } |
| RAPS | { <i>C</i> , <i>PTS</i> , <i>TAL</i> } | { <i>IEC</i> , <i>C</i> , <i>PTS</i> , <i>L</i> , <i>P</i> , <i>DCT</i> } | { <i>KL</i> , <i>B</i> , <i>S</i> , <i>LL</i> } | { <i>B</i> , <i>KL</i> , <i>S</i> , <i>KR</i> } |
| Rand RAPS | { <i>C</i> , <i>PTS</i> , <i>TAL</i> } | { <i>C</i> , <i>PTS</i> , <i>L</i> , <i>P</i> , <i>DCT</i> } | { <i>KL</i> , <i>S</i> , <i>LL</i> } | { <i>KL</i> , <i>S</i> , <i>KR</i> } |
| CPSN | { <i>PTS</i> , <i>TAL</i> } | { <i>C</i> , <i>PTS</i> , <i>DCT</i> } | { <i>S</i> , <i>LL</i> } | { <i>S</i> , <i>KR</i> } |

Table 2: A qualitative comparison of the conformal sets of CPSN vs. the tested baselines. Random samples were taken from the test fold, and the ground true classes are marked in green.

evaluation of the prediction sets on a given test set are set size (average length of prediction sets where a small value means high efficiency) and marginal coverage rate (fraction of testing examples for which the prediction sets contain the ground-truth labels). These two evaluation metrics can be formally defined as:

$$\text{size} = \frac{1}{n_{\text{test}}} \sum_i |C(x_i)|$$

$$\text{coverage} = \frac{1}{n_{\text{test}}} \sum_i \mathbf{1}(y_i \in C(x_i))$$

such that n_{test} is the size of the test set.

Implementation details. Each dataset was divided into train/validation/test folds of 80%/10%/10%. The first fold is used for training the regression network, the second for conformalization, and the third for evaluation (see Algorithm Box 1). Temperature Scaling [5] was used to calibrate the predicted class probabilities. APS was used to compute conformal scores for the training and validation sets. The regression network q consists of a two-layered MLP with ReLU activation. As input, it receives a representation of 2048 dimensions and is optimized in order to predict the conformal score. Each network was trained for 100 epochs using AdamW optimizer [15] with a learning rate of $5e - 4$, weight decay of $1e - 6$ and a batch size of 128. After convergence, the validation set is used for calculating the bias correction $\delta_{q(x)}$. The results are reported over the test fold. We repeat each experiment 10 times using different train/validation/test split seeds.

Table 1 presents a summary of the experimental results. We report the mean and the standard deviation of 10 experiments for each setup for $\alpha = 0.1$ and for $\alpha = 0.05$. As can be seen, the coverage requirement was fulfilled by all the methods including ‘naive’. On average, CPSN produces small prediction sets with low variance for all the setups evaluated. The

randomized versions of APS and RAPS yields better results than the deterministic versions. The RAPS algorithm became effective when the number of classes and the size of the prediction sets were both very large. As medical imaging classification tasks typically involve a moderate number of classes, APS and RAPS perform similarly. The bias correction values δ_1 and δ_2 in the case of TissueMNIST were 0.052 ± 0.15 . and 0.134 ± 0.17 . This empirical evidence highlights the need to calculate the conformal bias correction separately for each of the two sets.

Table 2 presents a qualitative comparison of a few samples from the two datasets along with the prediction sets produced by CPSN and the baseline methods. It is evident that CPSN generates smaller prediction sets, even for the challenging samples, while maintaining a high coverage rate.

5. CONCLUSIONS

We presented a method that allows us to take any classifier network and generate predictive sets that are guaranteed to achieve a pre-specified error level, while maintaining a small average size. The main novelty of our approach, in comparison to previous CP methods, lies in the utilization of a sample-based threshold to form the prediction set which is computed by a network. In this study, we focused on the task of medical diagnostics based on medical images. Prediction sets are particularly valuable for medical doctors since they make it possible to eliminate numerous possibilities and promptly refer the patient to the right specialists. Our method, however, is versatile and can be applied to other critical tasks.

6. COMPLIANCE WITH ETHICAL STANDARDS

This research study was conducted retrospectively using human subject data made available in open access by (Source

information). Ethical approval was not required as confirmed by the license attached with the open access data.

7. REFERENCES

- [1] Vladimir Vovk, Alexander Gammerman, and Glenn Shafer, *Algorithmic learning in a random world*, vol. 29, Springer, 2005.
- [2] Anastasios N. Angelopoulos and Stephen Bates, “Conformal prediction: A gentle introduction,” *Foundations and Trends in Machine Learning*, vol. 16, no. 4, pp. 494–591, 2023.
- [3] Charles Lu, Andréanne Lemay, Ken Chang, Katharina Höbel, and Jayashree Kalpathy-Cramer, “Fair conformal predictors for applications in medical imaging,” in *Proceedings of the AAAI Conference on Artificial Intelligence*, 2022.
- [4] Charles Lu, Anastasios N Angelopoulos, and Stuart Pomerantz, “Improving trustworthiness of AI disease severity rating in medical imaging with ordinal conformal prediction sets,” in *International Conference on Medical Image Computing and Computer-Assisted Intervention (MICCAI)*, 2022.
- [5] Chuan Guo, Geoff Pleiss, Yu Sun, and Kilian Q Weinberger, “On calibration of modern neural networks,” in *International Conference on Machine Learning (ICML)*, 2017.
- [6] Jeremy Nixon, Michael W Dusenberry, Linchuan Zhang, Ghassen Jerfel, and Dustin Tran, “Measuring calibration in deep learning,” in *CVPR Workshops*, 2019.
- [7] Yaniv Romano, Matteo Sesia, and Emmanuel Candes, “Classification with valid and adaptive coverage,” *Advances in Neural Information Processing Systems*, 2020.
- [8] Anastasios Angelopoulos, Stephen Bates, Jitendra Malik, and Michael I Jordan, “Uncertainty sets for image classifiers using conformal prediction,” *International Conference on Learning Representations (ICLR)*, 2021.
- [9] Bat-Sheva Einbinder, Yaniv Romano, Matteo Sesia, and Yanfei Zhou, “Training uncertainty-aware classifiers with conformalized deep learning,” in *Advances in Neural Information Processing Systems (NeurIPS)*, 2022.
- [10] Jiancheng Yang, Rui Shi, and Bingbing Ni, “MedMNIST classification decathlon: A lightweight automl benchmark for medical image analysis,” in *The IEEE International Symposium on Biomedical Imaging (ISBI)*, 2021.
- [11] Jiancheng Yang, Rui Shi, Donglai Wei, Zequan Liu, Lin Zhao, Bilian Ke, Hanspeter Pfister, and Bingbing Ni, “MedMNIST v2-a large-scale lightweight benchmark for 2D and 3D biomedical image classification,” *Scientific Data*, vol. 10, no. 1, pp. 41, 2023.
- [12] Patrick Bilic, Patrick Christ, Hongwei Bran Li, Eugene Vorontsov, Avi Ben-Cohen, Georgios Kaissis, Adi Szeskin, Colin Jacobs, Gabriel Efrain Humpire Mamani, Gabriel Chartrand, et al., “The liver tumor segmentation benchmark (lits),” *Medical Image Analysis*, vol. 84, pp. 102680, 2023.
- [13] Andre Woloshuk, Suraj Khochare, Aljohara F Almulhim, Andrew T McNutt, Dawson Dean, Daria Barwinska, Michael J Ferkowicz, Michael T Eadon, Katherine J Kelly, Kenneth W Dunn, et al., “In situ classification of cell types in human kidney tissue using 3D nuclear staining,” *Cytometry Part A*, vol. 99, no. 7, pp. 707–721, 2021.
- [14] Kaiming He, Xiangyu Zhang, Shaoqing Ren, and Jian Sun, “Deep residual learning for image recognition,” in *Proc. of the IEEE Conference on Computer Vision and Pattern Recognition (CVPR)*, 2016.
- [15] Ilya Loshchilov and Frank Hutter, “Decoupled weight decay regularization,” *arXiv preprint arXiv:1711.05101*, 2017.